Coherent phonon generation and the two stimulated Raman tensors

T. E. Stevens,[1,2,*] J. Kuhl,[2] and R. Merlin[1]
[1]*The Harrison M. Randall Laboratory of Physics, The University of Michigan, Ann Arbor, Michigan 48109-1120*
[2]*Max-Planck-Institut für Festkörperforschung, D-70569, Stuttgart, Germany*
(Received 22 January 2002; published 28 March 2002)

We show that stimulated Raman scattering by phonons is described by two separate tensors, one of which accounts for the phonon-induced modulation of the susceptibility, and the other one for the dependence of the coherent mode amplitude on the light intensity. These tensors have the same real component, associated with impulsive generation of phonons, but different imaginary parts. If the imaginary term dominates, the mechanism for two-band processes is displacive in nature. Femtosecond pump-probe experiments on antimony, using laser energies in the range of the E_2' gap, support the two-tensor model.

DOI: 10.1103/PhysRevB.65.144304 PACS number(s): 78.30.−j, 42.65.Dr, 42.65.Re, 78.47.+p

The Raman effect is historically associated with the spontaneous scattering of light by optical phonons in solids and molecular vibrations.[1] Discovered accidentally long ago,[2] stimulated Raman scattering (RS) has become an important subfield of nonlinear optics[3] as well as a valuable tool for vibrational spectroscopy.[4] Following recent developments in femtosecond laser technology, there has been considerable interest in the properties of the coherent vibrational fields that accompany stimulated RS processes, along with the exploration of alternative models for generating high-amplitude phonons.[5] While there is widespread agreement that RS is the key generation mechanism in the transparent region, its role in opaque materials has remained controversial.[6–8] Here we demonstrate a previously unrecognized feature of RS that can help settle the discussion.[9] Specifically, we prove that stimulated RS is defined not by one but two distinct tensors. The first one, χ_{kl}^R, is the standard Raman susceptibility discussed in textbooks[3] which gives both the modulation of the linear susceptibility by the phonon and the cross section for spontaneous RS. The second, new tensor π_{kl}^R characterizes the electrostrictive force acting on the ions. Consistent with the common understanding of stimulated Raman processes, the real parts of these tensors are identical and, thus, they become one and the same in the domain of transparency. Relevant to the absorbing region, however, their imaginary components differ appreciably. We have tested these predictions by examining the behavior of coherent phonons generated at photon energies in the range of the E_2' critical point of Sb. The experimental results are in very good agreement with the two-tensor model.

In the semiclassical formulation of stimulated RS, the interaction between the light and a single nondegenerate mode of the vibrational field is given by the phenomenological potential $V=-Nv_c\Sigma_{kl}\mathcal{R}_{kl}E_kE_lQ/2$.[3] Here N is the number of cells, v_c is the cell volume, $E_u(t)$ is a component of the electric field at time t,[10] Q is the phonon coordinate, $\mathcal{R}_{kl}\approx\partial\chi_{kl}/\partial Q$ is the Raman tensor, and χ_{kl} is the linear susceptibility. Let Ω_0 be the phonon frequency corresponding to a wave vector near the center of the Brillouin zone. Within the harmonic approximation, V leads to coupled phonon-photon field equations of the form

$$P_k=\sum_l \chi_{kl}E_l+P_k^R, \quad P_k^R=\sum_l \mathcal{R}_{kl}QE_l, \tag{1}$$

$$\ddot{Q}+\Omega_0^2Q=F(t)\equiv Nv_c\sum_{kl}(\mathcal{R}_{kl}E_kE_l)/2,$$

in which a single tensor is used to describe both the phonon-induced component of the polarization **P** and the electrostrictive force F driving the oscillator. These expressions are rigorously valid only if $\mathcal{R}_{kl}$ does not depend on frequency, but they can be modified without difficulty to account for dispersion. However, they cannot be used in absorbing media because the electromagnetic energy density is ill defined in the presence of dissipation.

To obtain results that apply for arbitrary $\mathbf{E}(t)$, we treat the electromagnetic field as classical, and consider the Hamiltonian

$$\hat{H}=\frac{1}{2}\hat{P}^2+\frac{\Omega_0^2}{2}\hat{Q}^2+\hat{H}_e-\hat{\Xi}\hat{Q}-\hat{\mathbf{\Delta}}\cdot\mathbf{E}(t), \tag{2}$$

where $\hat{Q}$ and $\hat{P}$ are the phonon coordinate and its associated momentum operator; $\hat{H}_e$ is the Hamiltonian of the electron subsystem with $\hat{H}_e|n\rangle=\hbar\omega_n|n\rangle$. The electron-phonon and electron-radiation interaction are given by $-\hat{\Xi}\hat{Q}$ and $-\hat{\mathbf{\Delta}}\cdot\mathbf{E}$,[11] where $\hat{\Xi}$ and the dipole-moment operator $\hat{\mathbf{\Delta}}$ depend only on electron variables.[12] From Eq. (2) we obtain $d^2\langle\hat{Q}\rangle/dt^2+\Omega_0^2\langle\hat{Q}\rangle=F\equiv\langle\hat{\Xi}\rangle$ where $\langle\cdots\rangle$ denotes the expectation value.[7,8] Let $F(\Omega)$ be the Fourier transform of $F(t)$. Then

$$\lim_{t\to\infty}\langle\hat{Q}(t)\rangle=\frac{-i}{\sqrt{8\pi}\Omega_0}[e^{i\Omega_0t}F(-\Omega_0)-e^{-i\Omega_0t}F(\Omega_0)]. \tag{3}$$

It follows that a real $F(\Omega)$ gives $\langle\hat{Q}(t)\rangle\propto\sin\Omega_0t$. This case, applying to below-gap excitation, encompasses that of a driving force of the impulsive type, i.e., $F(t)\propto\delta(t)$. If, instead, $F(\Omega)$ is purely imaginary we have a steplike, displacive-type excitation with $\langle\hat{Q}(t)\rangle\propto\cos\Omega_0t$.[5–8]

Using the density-matrix formalism, we obtain the familiar Raman correction to the polarization,[3]

$$\mathbf{P}^R(t) \equiv \frac{\langle \boldsymbol{\Delta} \rangle^R}{N v_c}$$

$$= \frac{1}{2\pi\hbar^2 N v_c} \sum_{mn} \int_{-\infty}^{+\infty} d\omega \int_{-\infty}^{+\infty} d\Omega e^{-i(\omega-\Omega)t} Q^*(\Omega)$$

$$\times \left\{ \frac{\Xi_{mn} \boldsymbol{\Delta}_{0m} |\boldsymbol{\Delta}_{n0} \cdot \mathbf{E}(\omega)|}{(\omega_m - i\gamma_m - \omega + \Omega)(\omega_n - i\gamma_n - \omega)} \right.$$

$$+ \frac{\Xi_{n0} \Delta_{0m} |\boldsymbol{\Delta}_{mn} \cdot \mathbf{E}(\omega)|}{(\omega_m - i\gamma_m - \omega + \Omega)(\omega_n - i\gamma_n + \Omega)}$$

$$\left. + \frac{\Xi_{0n} \boldsymbol{\Delta}_{nm} |\boldsymbol{\Delta}_{m0} \cdot \mathbf{E}(\omega)|}{(\omega_m - i\gamma_m - \omega)(\omega_n + i\gamma_n - \Omega)} \right\} + \text{c.c.}, \tag{4}$$

where $Q(\Omega)$ and $\mathbf{E}(\omega)$ are the Fourier transforms of $\langle \hat{Q}(t) \rangle$ and $\mathbf{E}(t)$, and γ_n is the decay rate of the nth state. To lowest order in $\mathbf{E}$, the same procedure gives the driving force:[8]

$$F(t) \equiv \langle \hat{\Xi} \rangle = \frac{1}{2\pi\hbar^2} \sum_{mn} \int_{-\infty}^{+\infty} d\omega \int_{-\infty}^{+\infty} d\Omega e^{-i\Omega t}$$

$$\times \left\{ \frac{1}{2} \frac{\Xi_{mn} [\boldsymbol{\Delta}_{n0} \cdot \mathbf{E}(\omega)][\boldsymbol{\Delta}_{0m} \cdot \mathbf{E}^*(\omega - \Omega)]}{(\omega_m + i\gamma_m - \omega + \Omega)(\omega_n - i\gamma_n - \omega)} \right.$$

$$\left. + \frac{\Xi_{0m} [\boldsymbol{\Delta}_{mn} \cdot \mathbf{E}(\omega)][\boldsymbol{\Delta}_{n0} \cdot \mathbf{E}^*(\omega - \Omega)]}{(\omega_m - i\gamma_m - \Omega)(\omega_n - i\gamma_n + \omega - \Omega)} \right\} + \text{c.c.} \tag{5}$$

Finally, we introduce the tensors χ^R_{kl} and π^R_{kl} by writing Eqs. (4) and (5) as

$$P^R_k(t) = \frac{1}{2\pi} \sum_l \int_{-\infty}^{+\infty} \int_{-\infty}^{+\infty} e^{-i(\omega-\Omega)t} \chi^R_{kl}(\omega, \omega - \Omega)$$

$$\times E_l(\omega) Q^*(\Omega) d\omega \, d\Omega \tag{6}$$

and

$$F(t) = \frac{N v_c}{4\pi} \sum_{kl} \int_{-\infty}^{+\infty} \int_{-\infty}^{+\infty} e^{-i\Omega t} E_l(\omega) \pi^R_{kl}(\omega, \omega - \Omega)$$

$$\times E^*_k(\omega - \Omega) d\omega \, d\Omega, \tag{7}$$

From Eqs. (4)–(7), we find immediately that $\chi^R_{kl} \equiv \pi^R_{kl} \equiv \mathcal{R}_{kl}(\omega, \omega - \Omega)$ if the decay rates exactly vanish. Hence, in agreement with Eq. (1), the tensors are identical in transparent materials and, more generally (i.e., even in the presence of absorption), we have $\mathrm{Re}(\chi^R_{kl}) \equiv \mathrm{Re}(\pi^R_{kl})$ in the limit $\gamma_n \to 0$. On the other hand, it is apparent that the imaginary components are not the same because the corresponding poles in Eqs. (4) and (5) are not in the same half of the complex plane.

To provide a physical picture of the previous results, we focus on the first terms of Eqs. (4) and (5) containing two resonant denominators, and consider the resonant contributions of two-band processes. Under the simplifying assumption $\Xi_{mn} \approx \Xi_0 \equiv \text{const}$, the Raman tensors can be written in terms of the linear dielectric tensor $\varepsilon_{ij}(\omega)$.[13] For $\gamma_n \to 0$ and also $|\Omega/\omega| \ll 1$, we obtain

$$\chi^R(\omega, \omega + \Omega) \approx \frac{\Xi_0}{4\pi\hbar\Omega} [\varepsilon(\omega + \Omega) - \varepsilon(\omega)]$$

$$\approx \frac{\Xi_0}{4\pi\hbar} \left[\frac{d\,\mathrm{Re}(\varepsilon)}{d\omega} + i \frac{d\,\mathrm{Im}(\varepsilon)}{d\omega} \right] \tag{8}$$

and

$$\pi^R(\omega + \Omega, \omega) \approx \frac{\Xi_0}{4\pi\hbar\Omega} [\varepsilon(\omega + \Omega) - \varepsilon^*(\omega)]$$

$$\approx \frac{\Xi_0}{4\pi\hbar} \left[\frac{d\,\mathrm{Re}(\varepsilon)}{d\omega} + 2i\,\mathrm{Im}(\varepsilon)/\Omega \right], \tag{9}$$

where the tensor indices have been omitted for simplicity.[14] As anticipated, these equations reveal significant differences between the imaginary components of the two Raman tensors. Assuming that $\varepsilon(\omega)$ varies slowly within the width of the pulses, from Eqs. (9) and (7) we obtain

$$F(\Omega) \propto \left[\frac{d\,\mathrm{Re}(\varepsilon)}{d\omega} + 2i\,\mathrm{Im}\,\varepsilon/\Omega \right] \int_{-\infty}^{+\infty} e^{i\Omega t} |E(t)|^2 dt. \tag{10}$$

Consistent with the discussion following Eq. (3), the real part of ε leads to $F(t) \propto |E(t)|^2$, whereas the imaginary term gives $F(t) \propto \int_{-\infty}^{t} |E(t')|^2 dt'$ which is displacive in character. Since $|d\,\mathrm{Re}(\varepsilon)/d\omega| \ll \mathrm{Im}(\varepsilon)/\Omega_0$ (this, not too close to the absorption edge or in the vicinity of a sharp exciton or impurity resonance), we expect that coherent phonons generated through two-band scattering will exhibit mainly a displacive behavior. The reason why the imaginary component of ε leads to a steplike force is simply the fact that, in the presence of absorption, the phonons couple to real charge-density fluctuations which live at least for a few phonon periods, and instantaneously shift the equilibrium position of the ions.[7,8] The driving force component that is in phase with the light pulse reflects coupling to virtual electronic transitions.

For various reasons, the E_2' critical point of Sb at $\sim$2 eV is ideally suited to test the two-tensor model.[15] Here a feature of interest is that the measured amplitude of the coherent phonon oscillations are surprisingly large for a material that is highly absorbing and does not exhibit very strong spontaneous RS.[6] Our two-tensor model solves this problem by relating the phonon amplitude to π^R, whose magnitude at $\sim$2 eV is a factor of $\sim$60 larger than that of χ^R.[15] Central to our choice were the facts that the spontaneous RS cross section at E_2' is dominated by two-band processes, as described by Eqs. (8) and (9), and that the width of the resonance is sufficiently large for Eq. (10) to apply.[16] It also helps that the optical parameters of Sb entering Eqs. (8) and (9) have very different magnitudes, with values $d\,\mathrm{Re}(\varepsilon)/d\omega \sim 5$–$10\ \mathrm{eV}^{-1}$, $d\,\mathrm{Im}(\varepsilon)/d\omega \sim 20$–$40\ \mathrm{eV}^{-1}$, and $2\,\mathrm{Im}(\varepsilon)/\Omega_0 \sim 1250$–$2500\ \mathrm{eV}^{-1}$ (Ref. 15) that sustain excitations of the displacive kind.[17] Within this framework, we recall that early ultrafast data on Sb and, in particular, the pioneering work using a colliding-pulse mode-locked laser resonant with E_2', revealed displacive-like oscillations as well as a discrepancy between spontaneous and coherent results for the relative behavior of the two Raman-active modes.[6] This led to the

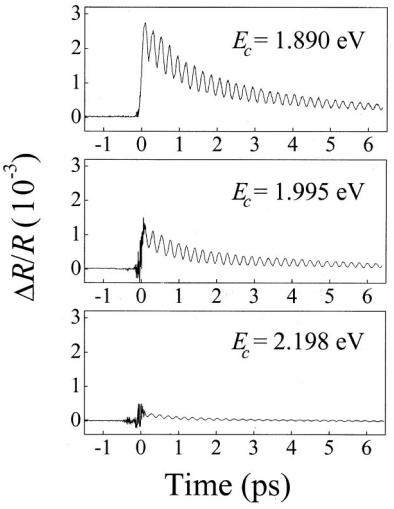

FIG. 1. Resonant normalized differential reflectivity for Sb at 300 K. The incident pump energy density is 120 μJ/cm^2. E_C is the central energy of the pulses which are polarized perpendicular to the trigonal axis. The data show coherent A_{1g} phonon oscillations of frequency $\Omega_0 \sim 4.5$ THz and a slowly varying electronic background. The fine structure near zero delay is due to interference between overlapping pump and probe beams.

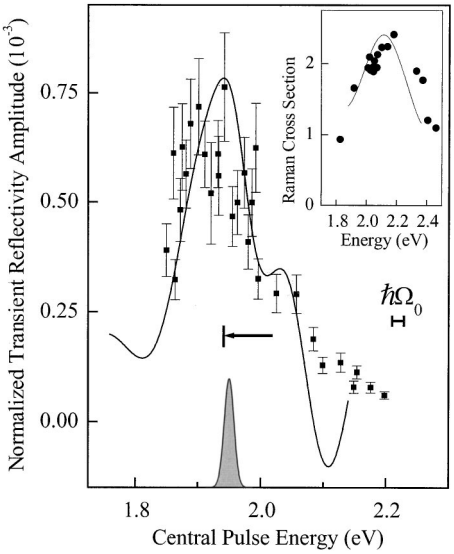

FIG. 2. Measured (■) amplitude of the A_{1g} oscillation as a function of E_C. The average incident powers of the pulses are ~2 mW (pump) and ~0.8 mW (probe). Error bars primarily reflect corrections due to the dependence of the amplitude on the pulse width; see Eq. (12). The solid line is a fit to Eq. (11) using dielectric constants gained from measurements on the same sample. As indicated by the arrow, the theoretical curve was shifted to lower energies by ~80 meV. The curve with shaded area at $E_C \approx 1.95$ eV represents the power spectrum of the pulses. Inset: measured (●) spontaneous RS cross section (arbitrary units) as a function of laser energy (Ref. 16) and fit (solid line) using Eq. (8) and optical data from Ref. 15.

belief that the generation mechanism in Sb (and other materials[6,7]) was not stimulated RS, but an alternative model named *displacive excitation* of coherent phonons (DECP). However, it was shown later that the ratio between the coherent-phonon amplitudes of the two Sb modes is actually very close to their RS intensity ratio.[8] The notion that DECP is not a distinct mechanism, but a particular case of stimulated RS was first proposed in Ref. 8.

The experiments were performed on a single crystal of antimony at room temperature using a cleaved surface oriented perpendicular to the trigonal axis. Sb has two Raman-active phonons of symmetries A_{1g} (totally symmetric) and E_g (doubly degenerate).[16] In this work, we focus on the dominant fully symmetric mode at ~4.5 THz.[6,8] Data were obtained using a standard pump-probe setup in the reflection geometry. The pump pulse creates the coherent phonon field associated with the A_{1g} mode which, in turn, leads to a change in reflectivity ΔR that we measured with the probe pulse as a function of the pump-probe delay using heterodyne detection.[17] As light source, we used an optical parametric amplifier (OPA) pumped by a 200-kHz Ti:sapphire regenerative amplifier. The OPA produces ~50 nJ 140 $\pm$25-fs pulses. The pulse central energy E_C can be tuned from ~1.8 to 2.3 eV to cover the range of the E_2' resonance. The reflected probe beam was spectrally integrated. The pump and probe beams had average powers of 2 and 0.8 mW and focal diameter sizes of 100 and 70 μm, respectively, and their polarizations were perpendicular to each other.

A representative set of our results revealing strong resonant behavior is shown in Fig. 1. In these traces, the probe beam differential reflectivity is plotted as a function of the time delay between the pump and probe pulses [at E_2', the reflectivity is ≈70% (Ref. 15)]. Figure 2 shows the E_C dependence of the amplitude of the oscillatory component of the signal, which we acquired from a fitting procedure that separates the phonon from the electronic contribution.[17] The theoretical curve was obtained from the two-band expressions neglecting the much weaker real component of Eq. (9). Using Ξ_0 as an adjustable parameter, we fit the experiments to

$$\Delta R/R \approx \frac{1}{R}\frac{\partial R}{\partial E_C} \times Q_0 \Xi_0, \tag{11}$$

where (even pulse)

$$Q_0 \approx \frac{\mathrm{Im}(\varepsilon) N v_c \Xi_0}{4\pi\hbar\Omega_0^2} \int_{-\infty}^{+\infty} e^{i\Omega_0 t} |E(t)|^2 dt \tag{12}$$

is the coherent phonon amplitude at the crystal surface.[17] Values of $\partial R/\partial E_C$ were gained from ellipsometry measurements conducted on the same sample.[18] Supporting our two-tensor model, theory and experiment show very good agreement. However, we find that there is a shift of ~80 meV between the E_2' peak in the resonant profile and the calculation based on the measured $\varepsilon(\omega)$. This behavior is reminiscent of resonant RS data where shifts of similar magnitude have been reported but remain poorly understood.[19] From the fit, we obtain the deformation potential $(NM_0)^{1/2}\Xi_0 = (4.0 \pm 1.5)$ eV/Å, where M_0 is the Sb atomic mass. It is of interest to emphasize the fact that the measurements of ΔR probe a combination of both, χ^R and π^R, since the former

tensor enters in the expression for $\partial R/\partial E_C$ and the latter in that of Q_0. Instead, the spontaneous RS experiments, reproduced for comparison purposes in the inset of Fig. 2, probe only χ^R. However, the overall line shape of the stimulated resonant profile reflects primarily the energy dependence of χ^R because Im(ε) and, thus, Q_0 does not vary much with E_C.[15,17] Finally, it is useful to note that the overall resonant enhancement for spontaneous scattering is much weaker than that observed in our time-domain experiments, a fact that goes back to the dominance of the term $\propto \mathrm{Im}(\varepsilon)$ in Eq. (9).

We thank M. Cardona for valuable discussions, and L. Lastras for providing the ellipsometry data before publication. The work was supported by the National Science Foundation under Grant No. DMR 9876862 and by the AFOSR under Contract No. F49620-00-1-0328 through the MURI program.

*Present address: Veridian ERIM International, P.O. Box 134008, Ann Arbor, Michigan 48113-4008.

[1] See, e.g., *Raman Scattering in Materials Science*, edited by W. H. Weber and R. Merlin, Springer Series in Materials Science Vol. 42 (Springer, Berlin, 2000), and references therein.

[2] E. J. Woodbury and W. K. Ng, Proc. IRE **50**, 2367 (1962).

[3] Y. R. Shen, *Principles of Nonlinear Optics* (Wiley, New York, 1984).

[4] W. E. Bron, in *Coherent Optical Interactions in Semiconductors*, Vol. 330 of *NATO Advanced Study Institute, Series B: Physics*, edited by R. T. Phillips (Plenum, New York, 1994), p. 199; A. Labereau and W. Kaiser, Rev. Mod. Phys. **50**, 607 (1978).

[5] For reviews, see T. Dekorsy, G. C. Cho, and H. Kurz, in *Light Scattering in Solids VIII*, edited by M. Cardona and G. Güntherodt (Springer, Berlin, 2000); R. Merlin, Solid State Commun. **102**, 207 (1997); L. Dhar, J. A. Rogers and K. A. Nelson, Chem. Rev. **94**, 157 (1994).

[6] H. J. Zeiger, J. Vidal, T. K. Cheng, E. P. Ippen, G. Dresselhaus, and M. S. Dresselhaus, Phys. Rev. B **45**, 768 (1992).

[7] A. V. Kusnetsov and C. J. Stanton, Phys. Rev. Lett. **73**, 3243 (1994).

[8] G. A. Garrett, T. F. Albrecht, J. F. Whitaker, and R. Merlin, Phys. Rev. Lett. **77**, 3661 (1996); note that the time-domain data reported in this work are off-resonance.

[9] A preliminary account of this work was reported at the International Conference on Solid State Spectroscopy, Schwäbisch Gmünd, Germany, 1999 [T. E. Stevens, J. Hebling, J. Kuhl, and R. Merlin, Phys. Status Solidi B **215**, 81 (1999)].

[10] For simplicity, we ignore the spatial dependence of the electric field. This applies strictly to samples with dimensions that are small compared with the wavelength of light. More generally, the interaction involves a continuum of modes with wave vectors close to the Γ point of the Brillouin zone (Ref. 8).

[11] In infinite crystals, it is customary to use the so-called $\mathbf{p}\cdot\mathbf{A}$ instead of $\mathbf{r}\cdot\mathbf{E}$ coupling, since the electronic contribution to the dipole moment does not give well-defined matrix elements. However, the matrix elements of the *total* dipole moment are well defined, and can be used instead to remove any inconsistency [see, e.g., A. S. Barker and R. Loudon, Rev. Mod. Phys. **44**, 18 (1972)].

[12] Note that $\langle\hat{\Delta}\rangle\sim O(N)$, while $\langle\hat{Q}\rangle$, $\langle\hat{\Xi}\rangle\sim O(\sqrt{N})$. Also the matrix elements Ξ_{mn} are $O(1/\sqrt{N})$ and $\Delta_{mn}\sim O(1)$.

[13] See, e.g., M. Cardona, in *Light Scattering in Solids II*, edited by M. Cardona and G. Güntherodt, Topics in Applied Physics Vol. 50 (Springer, Berlin, 1982), Chap. 2.

[14] As written, Eqs. (8) and (9) pertain only to fully symmetric modes. However, the relationship between the two-band component of the Raman susceptibility and the dielectric tensor applies more generally to all Raman-allowed symmetries (Ref. 13).

[15] See M. Cardona and D. L. Greenaway, Phys. Rev. **133**, A1685 (1964).

[16] J. B. Renucci, W. Richter, M. Cardona, and E. Schönherr, Phys. Status Solidi B **60**, 299 (1973).

[17] T. E. Stevens, Ph.D. Thesis, University of Michigan, 2000.

[18] L. Lastras and M. Cardona (unpublished).

[19] W. Richter, *Resonant Raman Scattering in Semiconductors*, Springer Tracts in Modern Physics Vol. 78 (Springer, Berlin, 1976); M. Cardona, Phys. Status Solidi A **184**, 1 (2001).